

# Device Performance of Light-Emitting Diode with Poly(phenylenesulfidephenyleneamine) as a Promotor of Hole Injection

Y.-H. Tak and H. Bässler\*

*Institut für Physikalische Chemie, Kernchemie und Makromolekulare Chemie und Zentrum für Materialwissenschaften der Philipps-Universität, D-35032 Marburg, Germany*

J. Leuninger and K. Müllen

*Max-Planck-Institut für Polymerforschung, Ackermannweg 10, D-55021 Mainz, Germany*

*Received: February 11, 1998*

Charge carrier injection into and electroluminescence from single-layer, bilayer, and trilayer light-emitting diodes have been studied under cw and pulsed operation. The active materials were poly(phenylenesulfidephenyleneamine) (PPSA), poly(*p*-phenylphenylenevinylene) (PPPV), and a blend of oxadiazole and polystyrene. Owing to its low oxidation potential PPSA promotes hole injection from ITO into the emitting PPPV layer. The energy level structure of the trilayer assembly leads to an enhancement of electron injection owing to the accumulation of positive space charge and prevents sweep out of holes and electrons from the emitting PPPV layer. An external quantum efficiency of 1% has been measured with an aluminium cathode. Time-resolved electroluminescence studies yield information on the kinetics of charge carrier recombination.

## 1. Introduction

The optimization of charge carrier injection is a central endeavor of research into light emitting diodes (LEDs). Straight-forward consideration of the recombination kinetics of electrons and holes in an organic solid predicts that the stationary number of holes and electrons required for achieving unit recombination efficiency must both be balanced and no less than the capacitance charge (CV). Otherwise some fraction of the charge carriers will be discharged nonradiatively at the respective exit contact.<sup>1,2</sup> This condition is met if contacts are ohmic, i.e., each being able to sustain a unipolar space charge limited current in a diode carrying a noninjecting exit electrode. It requires energy barriers for charge injection from the electrodes to be small, i.e., on the order of 0.25 eV or less. In a single-layer device, this would place an upper limit on the optical HOMO–LUMO gap of the active material not much in excess of the work function difference of the electrodes, i.e., about 2 ... 2.5 eV for a pair of indium tin oxide (ITO) and calcium electrodes. One way to overcome this limitation is to use bi- or multilayer devices in which hole- and electron-transporting layers are chosen on the premise that internal energy barriers are established that inhibit charge carrier leakage toward the contacts, thereby enhancing the stationary charge carrier density in the device.<sup>3–6</sup> Charge carrier injection can be enhanced by inserting thin buffer layers with low oxidation/reduction potentials between the dielectric and the electrode.<sup>7–9</sup> The latter strategy imposes restrictions on the material side if the cell is to be fabricated by spin coating from solution rather than by vapor deposition. The former case requires sufficiently different solubility properties of the active materials in order to find a combination of mutual nonsolvents for spin coating.

In the present paper we report on a novel material, poly(phenylenesulfidephenyleneamine) (PPSA)<sup>10,11</sup> that combines a low oxidation potential with good film forming properties yet restricted solubility. In a single layer diode hole injection from

ITO turns out to be an efficient process. It will be shown that this property is retained in bi- or trilayer LEDs that otherwise would sustain much lower cell currents and, concomitantly, feature much smaller electroluminescence - efficiencies.

## 2. Experiments

The following diode structures were investigated, electrodes being ITO and aluminium (Al) in all cases: (i) a single layer of PPSA prepared by spin coating from THF solution, (ii) a spin-coated single layer of poly(phenylphenylenevinylene) (PPPV) employing chloroform as a solvent, (iii) a bilayer structure consisting of PPSA and PPPV, and (iv) a trilayer assembly combining PPSA, PPPV, and a 20% (by weight) blend of 2-(4-biphenyl)-5-(4-*tert*-butylphenyl)-1,3,4-oxadiazol (PBD) and polystyrene, the latter deposited from cyclohexane solution. The diodes were characterized via (i) the current voltage dependence recorded with a Keithley source measure unit, (ii) the electroluminescence intensity as a function of the applied voltage using a photomultiplier as a detector, and (iii) the photo- and electroluminescence spectra recorded with a OMA system. For the trilayer-LED the time response of the electroluminescence upon addressing the device with rectangular voltage pulses was studied in addition. All experiments were carried out at 295 K and at a pressure of 10<sup>−6</sup> mbar. External quantum efficiencies were determined with a calibrated radiometer setup.

## 3. Results

Figure 1 shows a series of  $j(F)$  characteristics measured with the four types of diodes described in the experimental section. The highest currents are observed with a PPSA single-layer device. Depending on the external electric field the current is 2–4 orders of magnitude lower if the active layer is PPPV. Substantial enhancement of the current can be achieved by inserting a PPSA layer between ITO and PPPV. At fields > 10<sup>6</sup> V cm<sup>−1</sup>, the enhancement effect is retained even if a hole-

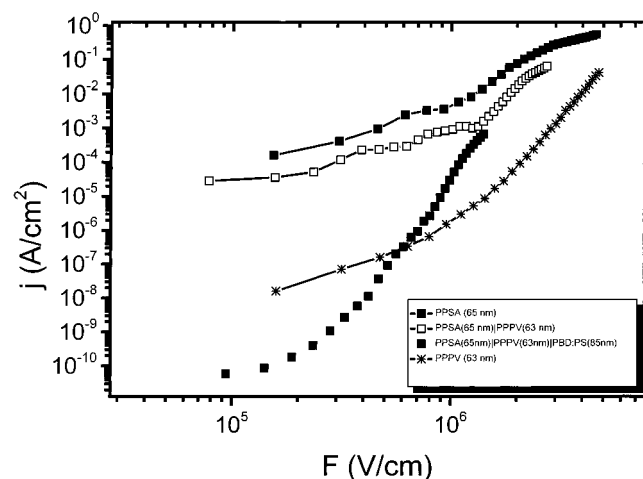


**Figure 1.**  $j(F)$  characteristics of the layer assemblies indicated in the inset. Electrodes were ITO (anode) and aluminium (cathode).

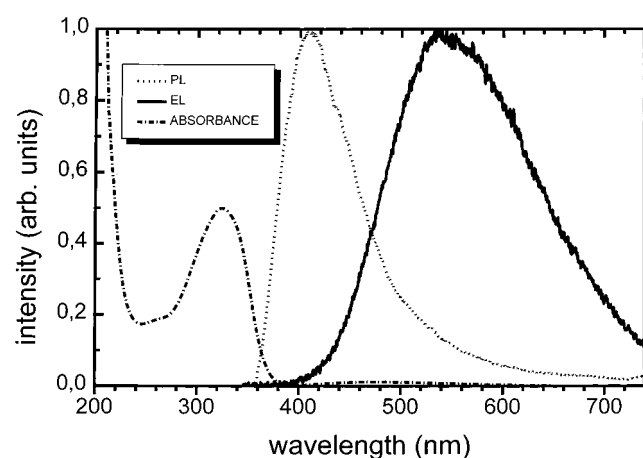


**Figure 2.** Absorption, photoluminescence, and electroluminescence spectra of PPSA.

blocking PBD (PS) layer is introduced, although the latter is known to screen the electric field at the anode because of the accumulation of positive space charge at the internal interface between the hole-transporting (PPPv) layer and the PBD (PS) layer. Electroluminescence (EL) is observed both from a PPSA single-layer device and from a PPSA|PPPv|PBD (PS) trilayer assembly. In the former case the EL spectra is significantly red-shifted compared to the photoluminescence (Figure 2). This is unusual, and no straightforward explanation can be offered. One possibility is that electroluminescence results mostly from electron-hole recombination involving a pair of adjacent polymer chains in sandwichlike topology that stabilizes a geminate e...h pair. Since for reasons discussed below this effect is irrelevant as far as multilayer LEDs are concerned, it will not be considered further. The EL-spectra of the trilayer device is characteristic of PPPv (Figure 3). Figure 4 illustrates the effect that the presence of the PPSA layer has on the external quantum efficiency  $\eta_{\text{ext}}$ . Inserting a PPSA layer between ITO and PPPv lowers the range of the electric field in which  $\eta_{\text{ext}}$  passes through a maximum by a factor of 2, while absolute values of  $\eta_{\text{ext}}$  are unaffected. Introduction of a cathodic PBD-(PS) layer causes  $\eta_{\text{ext}}$  to increase by 2 orders of magnitude and reach values of the order of 1%.

Onset of EL from a trilayer LED upon application of a rectangular step voltages is limited by the RC-time constant of the circuit, which is of the order of  $10 \mu\text{s}$ . No delay time is observed. Saturation of the EL-emission is attained after a rise

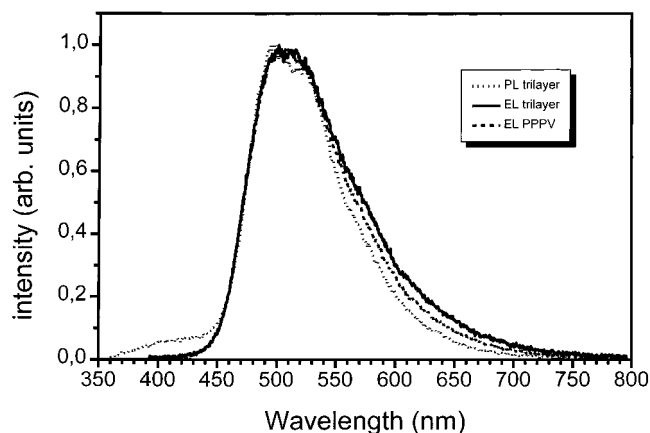


**Figure 3.** Electroluminescence and photoluminescence spectra of a PPSA|PPPv|PBD (PS) device. The EL-spectrum of a single-layer PPPv device is included for comparison.

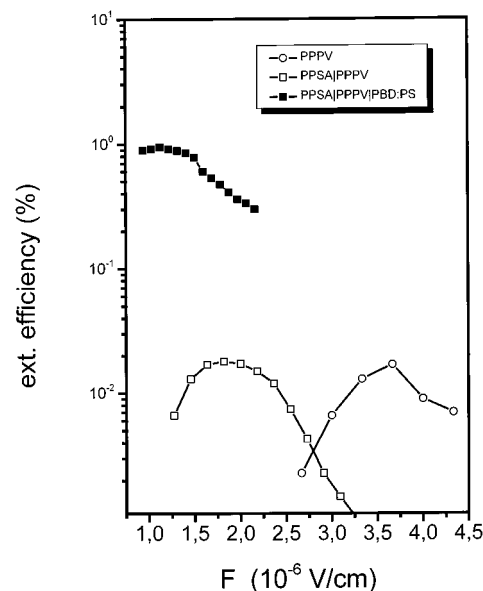


**Figure 4.** External electroluminescence quantum efficiencies of a single-layer PPPv diode, a PPSA|PPPv bilayer diode, and a PPSA|PPPv|PBD (PS) trilayer diode.

time of the order of 0.5 ms (Figure 5). At the falling edge of a rectangular voltage pulse an overshoot of the EL occurs whose magnitude depends on the pulse duration (Figure 6). The ratio of peak to cw-emission increases with decreasing external voltage (Figure 7). Plotting the decay of the EL-luminescence at the end of the voltage pulse on a double logarithmic scale reveals the nonexponential character of the decay process. After passing through a RC-limited maximum, the intensity decays in a power law fashion,  $I(t) \propto t^{-n}$ , with  $n = 1.25 \pm 0.05$  (Figure 8).

## 4. Discussion

**4.1. cw-Measurements.** In single-layer diodes of PPSA and PPPv with ITO anode and Al cathode, the majority charge carriers are holes injected from ITO. Comparing current field characteristics with theoretical predictions based upon a model developed for charge injection into a random organic hopping system<sup>12</sup> yields good agreement assuming hole injection barriers of  $\approx 0.3$  and  $0.6$  eV, respectively. (Figure 9) Taking the work function of ITO to be 4.8 eV results in average ionization potentials of 5.1 and 5.4 eV, respectively. The oxidation potential of PPSA relative to Ag/AgCl is  $-0.67$  V. By

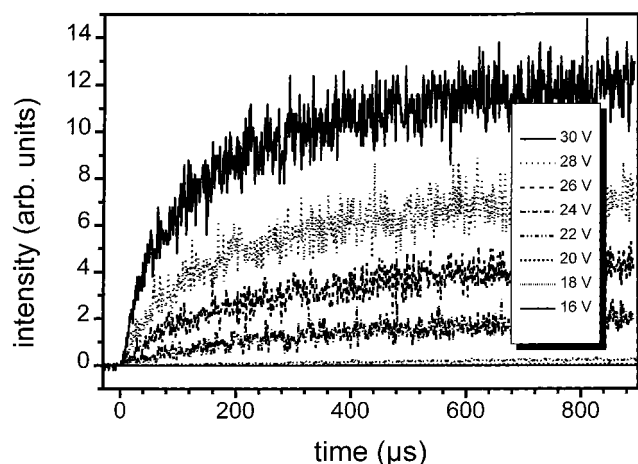


**Figure 5.** Onset of electroluminescence from a trilayer LED consisting of a 65 nm thick PPSA layer, a 63 nm thick PPPV layer, and a 85 nm thick PBD (PS) layer, sandwiched between ITO and Al electrodes, upon application of a rectangular voltage pulses. The load register was 500  $\Omega$ .

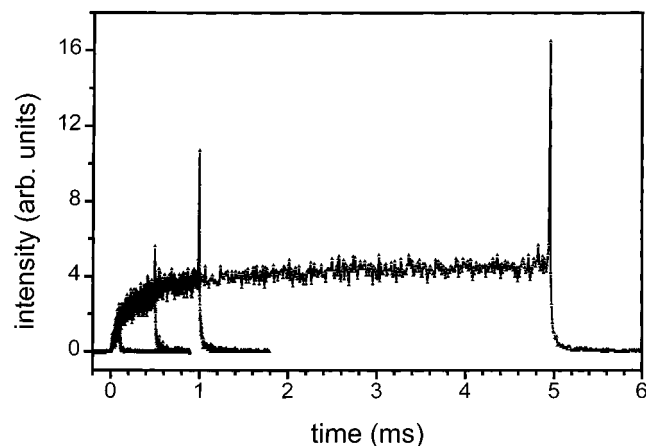


**Figure 6.** Time-resolved electroluminescence from the trilayer LED, described in Figure 5, upon applying 30 V pulses of 0.1, 0.5, 1, and 5 ms duration, respectively.

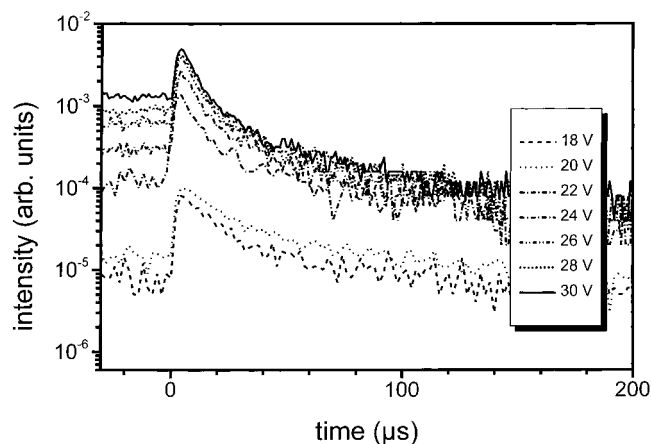


**Figure 7.** Decay of the electroluminescence signal of the end of a rectangular voltage pulse of 50 ms duration and variable amplitude. Note the logarithmic ordinate scale.

comparing oxidation potentials measured relative to a ferrocene/ferrocenium electrode (FOC) and to a Ag/AgCl electrode, respectively, one can derive a scaling relation  $E_{ox}(\text{Ag/AgCl}) = E_{ox}(\text{FOC}) - 0.4 \text{ eV}$ . Since the absolute energy of an FOC standard is  $-4.8 \text{ eV}$  below vacuum,<sup>6</sup> the above value translates into a HOMO position of PPSA at an energy  $-5.08 \text{ V}$  below

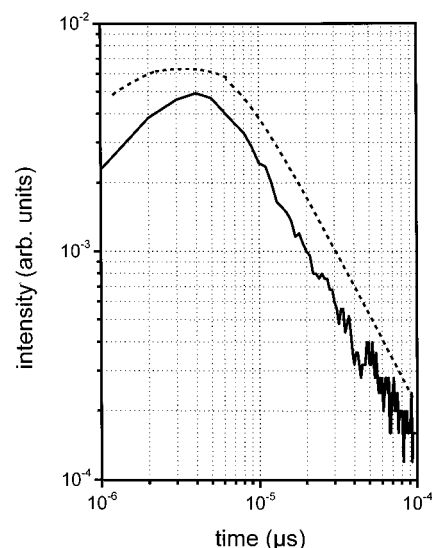


**Figure 8.** Decay of the electroluminescence intensity at the end of a rectangular voltage pulse in double logarithmic representation;  $t = 0$  refers to the end of the voltage pulse. The dashed curve is theoretical (from ref 24).

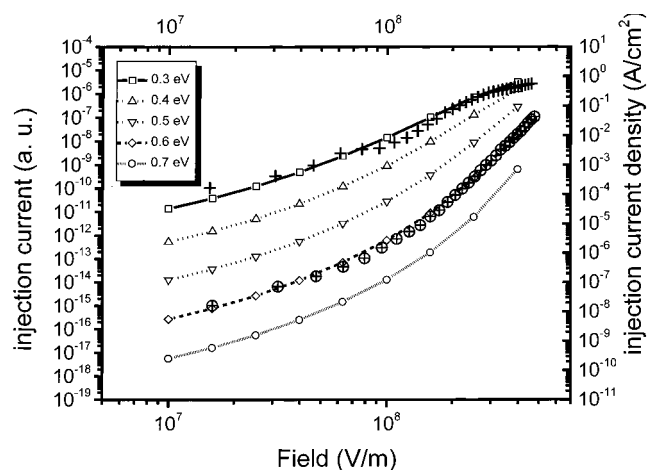


**Figure 9.** Comparison of the  $j(F)$  characteristics of ITO|PPSA|Al (crosses) and ITO|PPPV|Al (encircled crosses) diodes from Figure 1 with the prediction of the theory of ref 10 for injection-limited currents parametric in the zero-field injection barrier.

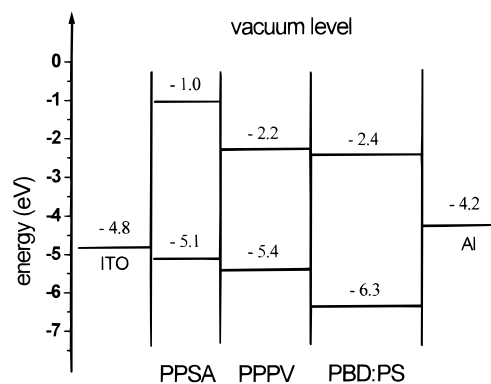


**Figure 10.** Energy level structure of the ITO|PPSA|PPPV|PBD (PS)|Al device.

This concurs with the above estimate derived from the  $j(F)$  characteristic. If combined with the known data for HOMO and LUMO position in PBD, one arrives at the energy level diagram for the trilayer assembly shown in Figure 10. The locations of the electron-transporting level of PPSA and PPPV have been derived from the optical gap, i.e., the energy of the

maximum of the  $S_1 \leftarrow S_0$  0–0 absorption band under the premise of the exciton binding energy being 0.4 eV.<sup>13</sup> Though associated with some uncertainty, this choice does not affect the main conclusion as far as the dominant internal energy barriers are concerned.

The question arises whether or not the ITO|PPSA|Al contact is ohmic, i.e., able to act as an unexhaustible reservoir of holes. If so, the hole-dominated current in a ITO|PPSA|Al diode should be space charge limited.<sup>14–16</sup> Although the current approaches a  $j \sim F^{1.6}$  law at high fields, which might be considered as an indication that Child's law is approximately fulfilled, there is independent evidence for current densities exceeding  $0.3 \text{ A cm}^{-2}$  being controlled by the serial resistance of ITO. For this reason and because of the agreement of the  $j(F)$  characteristic for  $j < 10^{-1} \text{ A cm}^{-2}$  with theoretical predictions, we are led to conclude that the injection barrier of 0.3 eV exceeds the upper limit for the electrode to be ohmic. Bearing in mind that the current, if space charge limited, were to follow Child's law, i.e.,  $j^{\text{SCL}} = (9/8)\epsilon\epsilon_0\mu F^2/d$ , one arrives at a lower bound for the effective hole mobility in PPSA, i.e.  $\mu_+ \geq 7 \times 10^{-7} \text{ cm}^2/\text{V s}$ .

An essential message of this work is that current flow across a ITO|PPSA|PPP|Al diode is essentially controlled by the anodic energy barrier, i.e., by the energetic position of the hole-transporting level of the layer on top of the ITO rather than that of the layer to follow. The likely reason why current flow will not ultimately be controlled by the sum of the anodic and the internal energy barriers for hole transport is that because of the finite thickness of the internal interface the latter barrier is more or less spatially smeared out and compensated by the potential drop due to the applied electric field.<sup>9</sup>

The situation changes in the presence of a third layer in between PPPV and Al that impedes hole transfer toward the cathode. It causes hole accumulation at that interface with concomitant enhancement of the cathodic electric field and of electron injection and, simultaneously, screening of the anodic field. However in view of the small barrier at the ITO|PPSA anode that screening effect vanishes at high fields, and the  $j(F)$  characteristic approaches that of the PPSA|PPP|Al bilayer system at high fields.

The important advantage of the trilayer assembly as compared to the system ITO|polythiophenevinylene|1,4-bis(4'-diphenylaminostyryl)-2,5-dimethoxybenzene|PBD(PS)|Al studied earlier<sup>9</sup> is the existence of large internal energy barriers for both hole flow from the intermediate PPPV layer toward the cathode and electron flow into the PPSA layer. At the same time the energy barrier for hole flow into the PPPV layer is small as is the barrier for electron transport from PBD into PPPV. This minimizes nonradiative, charge transfer-like interlayer recombination processes at internal interfaces and maximizes charge accumulation inside the PPPV while not impeding charge flow into the recombination zone. Evidence for recombination taking place exclusively in the central PPPV layer comes from the emission spectrum being characteristic of PPPV rather than of PPSA.

The functional shape of the field dependence of the external quantum efficiency is in accord with theory.<sup>17,18</sup> The increase at low fields is due to the steeper  $j(F)$  characteristic of minority (i.e., electron) injection as compared to majority carrier injection. At high electric field, sweep out effects become progressively important. The shift of the  $\eta_{\text{ext}}(F)$  curve toward lower electric fields upon inserting a PPSA layer between ITO and PPPV correlates with hole injection becoming more efficient. A given probability that an injected electron will encounter a hole to recombine with will therefore be established at lower fields

already. For the number of recombination events per injected majority carrier to stay constant, it is required, though, that the electron injection characteristics also experiences some shift toward lower fields, indicating that some internal charging must have occurred at the PPSA|PPP|Al interface. In both cases absolute efficiencies are of the order of  $10^{-2}\%$  only. The external efficiency rises up to 1% even with Al as a cathode upon introducing a cathodic PBD (PS) blocking layer. This is due to the coincidence of three favorable effects: (i) efficient hole injection due to the reduced anodic energy barrier, (ii) improved electron injection due to internal space charge accumulation, and (iii) charge confinement within the central emitting layer thereby minimizing carrier leakage toward the electrodes.

The theoretical external efficiency of a LED is  $\eta_{\text{ext}} = (1/4)\varphi_{\text{PL}}\varphi_{\text{rec}}(2n^2)^{-1}$  where  $\varphi_{\text{PL}}$  is the quantum efficiency of photoluminescence,  $(1/4)\varphi_{\text{rec}}$  is the probability that an injected majority carrier recombines with minority carriers to form a singlet state, and the factor  $(2n^2)^{-1}$  accounts for wave-guiding effects inside the LED if EL is recorded perpendicular to the cell normal.<sup>19</sup> From the fluorescence decay of  $\approx 200 \text{ ps}$ <sup>20</sup> as compared to a radiative lifetime of  $\approx 1.2 \text{ ns}$ ,<sup>21</sup>  $\varphi_{\text{PL}} = 0.16$  is obtained. Assuming an average refractive index of 1.6 for the trilayer assembly,  $2n^2 \approx 5$ . On the basis of this estimate, the measured external quantum efficiency would already have reached its upper limit set by the condition  $\varphi_{\text{rec}} = 1$ . Since it is unlikely that balanced injection can be realized with Al as a cathode, we conjecture that, in fact, more light is emitted perpendicular to the plane of the LED than predicted for an ideal wave-guiding system. One reason may be the roughness of the surface(s). In any case, this estimate indicates that both minority carrier injection as well as bimolecular charge carrier recombination must be highly efficient in a trilayer LED of the energy level structure shown in Figure 10.

**4.2. Time-Resolved Measurements.** Electroluminescence cannot commence until the leading edges of the injected distributions of electrons and holes begin to interpenetrate. Since PPSA and PPPV are present in the form of bulk films whereas PBD is incorporated into a binder, it is straightforward to assume that electron passage across the latter layer should determine the temporal onset of EL. From Figure 5 it is obvious that any delay time is masked by the RC time constant of the circuit, which is  $\approx 10 \mu\text{s}$ .  $\mu^- \geq 7 \times 10^{-7} \text{ cm}^2/\text{V s}$  follows for electron transport across a 85 nm thick PBD (PS) layer at an applied voltage of 24 V across a 213 nm thick sample. This value is by a factor of 7 larger than the electron mobility reported by Tokuhisa et al.<sup>22</sup> for a 20% dispersion of PBD in polycarbonate. There are several reasons for this discrepancy: (i) the electric field inside the device is about a factor of 2 larger than that used in the time of flight experiments of ref 22, (ii) use of the apolar polystyrene instead of polycarbonate reduces the energetic disorder a moving charge carrier experiences and, concomitantly, increases its mobility,<sup>23</sup> and (iii) the thickness of the PBD (PS) layer was only about  $1/50$  of that of the PBD (PC) layers used in ref 22. In a thin sample the mobility is supposed to be larger because the short drift time prevents carriers from relaxing to their equilibrium transport level.<sup>24</sup>

Subsequent rise of the EL-intensity occurs on a time scale of  $< 1 \text{ ms}$ . At an applied voltage of 30 V it is completed within  $400 \mu\text{s}$ . The amount of charge transported up to that time is  $3 \times 10^{-7} \text{ C/cm}^2$ . This is comparable to the capacitor charge of  $4.5 < 10^{-7} \text{ C/cm}^2$  calculated for a thickness of 213 nm, a dielectric constant  $\epsilon = 3$ , and  $V = 30 \text{ V}$ . This confirms (i) that the rise time is controlled by charge accumulation inside the

device, i.e., within the emitting PPPV layer and (ii) that the amount of stored charge is comparable to what the device can accommodate electrostatically.

At the end of the voltage pulse, the external component of the electric field at the electrodes decays to zero within the RC-time of the circuit. Injection is terminated but recombination persists until the reservoir of minority carriers is exhausted, albeit under different conditions from those under cw-operation conditions. During the on-stage of the applied voltage, the electric field inside the active PPPV layer is the sum of the external field and the (opposing) space charge field established by the charges that accumulate at the opposite sides of that layer. After turning off the external voltage, recombination is exclusively driven by the internal space charge field while carrier leakage across the internal interface is eliminated. The occurrence of the EL overshoot at the end of the voltage pulse is signature of this situation.<sup>25</sup> A quantitative theory<sup>26</sup> has been presented elsewhere. It is suffice to mention here that the evolution of the magnitude of the EL spike as a function of the duration of the voltage pulse maps growth of the charge carrier reservoir within the emitting layer.

Of interest is the decay of the EL after shortening the device because it yields information on the kinetics of charge carrier recombination inside the recombination zone. Replotting the signal as a function of the time on a double logarithmic scale with the origin of the time scale being set by the time at which the voltage has been turned off reflects the nonexponential character of the recombination process. For  $t > 10 \mu\text{s}$  a power law  $I(t) \propto t^{-1.25 \pm 0.1}$  is observed. This is a reflection of the dispersive character of charge carrier migration within a thin layer of the emitting PPPV. It is caused by the energetic disorder of PPPV-segments among which charge carrier hopping proceeds and which the large inhomogeneous width of the absorption profile is a manifestation of. Solving the equation for dispersion transport<sup>26</sup> yields the time dependence of the rate at which carriers are captured by tail states of the distribution. It decreases with time as  $p(t) = [\tau_0 \ln^3(\nu_0 t)]^{-1}$ ,  $\tau_0$  being the jump time of a carrier among a pair of isoenergetic sites and  $\nu_0$  the attempt to jump frequency, and is insensitive to the exact shape of the density of the states function. This is because a carrier can make only a few jumps, preferentially into energetically deeper states, before recombination occurs. Notice that  $3 \times 10^{-7} \text{ C/cm}^2$  (see above) within a 63 nm corresponds to a charge density of  $3 \times 10^{17} \text{ cm}^{-3}$  and to an average distance among charge carriers of about 15 nm only. Nikitenko et al.<sup>26</sup> have shown that the above time-dependent capture rate leads to a temporal decay of the number of recombination events of the form  $I(t) \propto [t \ln^4 \nu_0 t]^{-1}$ , which reproduces as  $I(t) \propto t^{-n}$  with  $n$  decreasing from  $\sim 1.3$  at shorter time to  $\sim 1.05$  at in the longtime limit. The shape of the theoretical  $I(t)$  profile is included in Figure 8. The agreement with experiment is striking. It is worth mentioning that a Monte Carlo simulation of the rate of geminate pair recombination in an energetically disordered hopping system yielded the same result,<sup>27</sup> indicating that in this case it makes no difference if recombination is of geminate or nongeminate type. In both cases it is the time-dependent diffusion toward target site that is rate-limiting.

## 5. Conclusion

Poly(phenylenesulfidephenyleneamine) has turned out to be a promising material for hole injection into multilayer LEDs.

It combines a low oxidation potential with a high LUMO required for preventing electron flows toward the anode. In a trilayer assembly an external quantum efficiency of 1% has been measured in a device with Al as a cathode although the emitter material, PPPV, has a photoluminescence quantum efficiency less than 20% because of excited-state quenching at nonfluorescent impurities. By optimizing the emitter material it should, therefore, be possible to achieve quantum efficiencies of commercial interest without using a highly corrosive calcium cathode.

**Acknowledgment.** Financial support by the Bundesministerium für Bildung Wissenschaft Forschung und Technologie (BMBF) as well from the Fonds der Chemischen Industrie is gratefully acknowledged. We are indebted to Dr. J. Oberski and Dr. A. Greiner for the preparation of PPPV.

## References and Notes

- (1) Albrecht, U.; Bässler, H. *Chem. Phys.* **1995**, *199*, 207.
- (2) Bässler, H.; Tak, Y.-H.; Khramtchenkov, D. V.; Nikitenko, V. R. *Synth. Met.* **1997**, *91*, 173.
- (3) Brown, A. R.; Burroughes, J. H.; Greenham, N. C.; Friend, R. H.; Bradley, D. D. C.; Burn, P. L.; Kraft, A.; Holmes, A. B. *Appl. Phys. Lett.* **1992**, *61*, 2793.
- (4) Bradley, D. D. C. *Synth. Met.* **1993**, *64*, 401.
- (5) Zhang, C.; Heger, S.; Pakbaz, K.; Wendl, F.; Heeger, A. J. *J. Electron. Mater.* **1994**, *23*, 453.
- (6) Pommerehne, J.; Vestweber, H.; Guss, W.; Mahrt, R. F.; Bässler, H.; Porsch, M.; Daub, J. *Adv. Mater.* **1995**, *7*, 551.
- (7) Doi, S.; Kuwabara, M.; Noguchi, T.; Ohnishi, T. *Synth. Met.* **1993**, *41*.
- (8) Antoniadis, H.; Hsieh, B. R.; Abkowitz, M. A.; Stolka, M. *Appl. Phys. Lett.* **1993**, *62*, 3167.
- (9) Tak, Y.-H.; Mang, S.; Greiner, A.; Bässler, H.; Pfeiffer, S.; Horhold, H. H. *Acta Polym.* **1997**, *48*, 450.
- (10) Wang, L.; Soczka-Guth, T.; Havinga, E.; Müllen, K. *Angew. Chem. Int. Ed. Engl.* **1996**, *35*, 1495.
- (11) Leuninger, J.; Wang, C.; Soczka-Guth, T.; Enkelmann, V.; Pakula, T.; Müllen, K. *Macromolecules* in press.
- (12) Arkhipov, V. I.; Emelianova, E. V.; Tak, Y.-H.; Bässler, H. *J. Appl. Phys.*, in press.
- (13) Barth, S.; Bässler, H. *Phys. Rev. Lett.* **1997**, *79*, 4445.
- (14) Blom, P. W. M.; de Jong, M. J. M.; Vleggar, J. J. M. *Appl. Phys. Lett.* **1996**, *68*, 3308.
- (15) Campbell, A. J.; Bradley, D. D. C.; Lidzey, D. G. *J. Appl. Phys.* **1997**, *82*, 000.
- (16) Pommerehne, J.; Selz, A.; Book, K.; Koch, F.; Zimmermann, F.; Unterlechner, C.; Wendorff, J. G.; Heitz, W.; Bässler, H. *Macromolecules* **1997**, *30*, 8270.
- (17) Khramtchenkov, D. V.; Arkhipov, V. I.; Bässler, H. *J. Appl. Phys.* **1997**, *81*, 6954.
- (18) Tak, Y.-H.; Bässler, H. *J. Appl. Phys.* **1997**, *81*, 6963.
- (19) Greenham, N. C.; Friend, R. H.; Bradley, D. D. C. *Adv. Mater.* **1994**, *6*, 491.
- (20) Lemmer, U.; Mahrt, R. F.; Wada, Y.; Greiner, A.; Bässler, H.; Gobel, E. O. *Appl. Phys. Lett.* **1993**, *62*, 2827.
- (21) Greenham, N. C.; Samuel, I. D. W.; Hayes, G. R.; Phillips, R. T.; Kessner, Y. A. R.; Moratti, S. C.; Holmes, A. B.; Friend, R. H. *Chem. Phys. Lett.* **1995**, *241*, 89.
- (22) Tokuhisa, H.; Era, M.; Tsutsui, T.; Saito, S. *Appl. Phys. Lett.* **1995**, *66*, 3433.
- (23) Borsenberger, P. M.; Bässler, H. *J. Chem. Phys.* **1991**, *25*, 5327.
- (24) Bässler, H. *Phys. Status Solidi B* **1993**, *175*, 15.
- (25) Tak, Y.-H.; Pommerehne, J.; Vestweber, H.; Sander, R.; Bässler, H.; Horhold, H.-H. *Appl. Phys. Lett.* **1996**, *69*, 1291.
- (26) Nikitenko, V. R.; Arkhipov, V. I.; Tak, Y.-H.; Pommerehne, J.; Bässler, H.; Hörhold, H.-H. *J. Appl. Phys.* **1997**, *81*, 7514.
- (27) Ries, B.; Bässler, H. *J. Mol. Electron.* **1987**, *3*, 15.